3-Picolyl and 2,5-Lutidyl Radicals: Generation, Optical Spectroscopy, and ab Initio Calculations

J. A. Bray and E. R. Bernstein*

Department of Chemistry, Colorado State University, Fort Collins, Colorado 80523-1872

Received: August 24, 1998; In Final Form: November 3, 1998

Electronic spectra are reported for two ring-substituted benzyl-like radicals, 3-picolyl and 2, 5-lutidyl. These pyridine-based radicals have much shorter excited state (D_1) lifetimes than their benzyl radical prototypes. The 3-picolyl radical (3-($\dot{C}H_2$)C_5H_4N) has an excited-state D_1 lifetime of ∼9 ns, and the 2,5-lutidyl radical (2-(CH_3),5-($\dot{C}H_2$)C_5H_3N) has an excited-state D_1 lifetime of ∼245 ns. The near-degeneracy of the D_1 and D_2 states of the benzyl radical is not found for these pyridine-based radicals, and the strong D_1-D_2 vibronic interaction is missing as well in these species. A number of ab initio calculations, at the (5 × 5) CASMP2 and (7 × 7) CAS levels with DZP and d95** basis sets, are employed to rationalize these results and assign the spectra. One possibility for the absence of other isomeric radical spectra is a rearrangement to a seven-membered radical ring form. The dynamics of radiationless transitions, ring expansion and rearrangement, and excited-state lifetimes are all factors for the spectroscopic detection of these radicals. Based on the calculations, the excited-state vibrational modes ν_{6a}, ν_{6b}, and ν_1 are assigned for the picolyl and lutidyl radicals.

Introduction

Electronic spectroscopy of the benzyl radical ($C_6H_5CH_2^{\bullet}$) has received a great deal of attention since the radical was first isolated more than 40 years ago.[1−6] Much of the interest in understanding the excited electronic states of the benzyl radical derives from the extensive vibronic coupling that occurs between the first two excited electronic states of this radical. The first two excited electronic states of the benzyl radical are suggested to lie within ∼800 cm^{-1} of one another and give rise to strong vibronic coupling:[4−6] both theoretical and experimental studies have explored this mixing. Expanded investigations of similar systems, such as *o*-, *m*-, and *p*-fluorobenzyl radicals[2] and *o*-, *m*-, and *p*-methyl benzyl radicals,[7] have assisted in deciphering the extent of this vibronic mixing.

An additional perturbation to the excited electronic states of the benzyl radical would be generated by substitution of one of the carbon atoms of the ring by a nitrogen atom. The behavior of benzene vs pyridine is a well-know comparison.[8−10] The S_1 excited state of pyridine has a very short lifetime compared to that of benzene (ca. 50 ps vs 100 ns) due to extremely rapid internal conversion, large intersystem crossing, and strong vibronic coupling between the S_0, S_1, S_2, and T_0 states of pyridine.

In this study, we investigate the properties of the radicals that arise through substitution of the benzene ring in benzyl radicals by a pyridine ring. The mass-resolved excitation spectra of two previously unreported radicals, 3-picolyl (3-($\dot{C}H_2$)C_5H_4N) and 2,5-lutidyl (2-(CH_3),5-($\dot{C}H_2$)C_5H_3N), are presented and discussed in this paper. Ab initio calculations are carried out to support the identification of the radical transitions. Transitions for 2- and 4-picolyl radicals are also calculated in an attempt to explain why these species remain unobserved. The second excited electronic state for 3-picolyl and 2,5-lutidyl radicals lies at much higher energy.

Experimental Procedures

The precursors used to generate the radicals in this study, 98% pure 3-methylpyridine (picoline) and 98% pure 2,5-dimethylpyridine (2,5-lutidine), are purchased from Aldrich and used as precursors as received. The compound samples are placed into a pulsed Jordan valve and heated ∼20 °C above room temperature to increase their vapor pressure. Only slight modifications are made to the photolysis setup described in ref 11. The first modification is the angle the photolysis laser beam makes with the molecular beam axis. This angle is changed from 45° to approximately 20°. By changing this angle, less laser power is needed for photolysis, ∼60 mJ/pulse using 193-nm photons, and the radical is accessible in the molecular beam for a longer period of time. The resulting signal improvements are due primarily to the photolysis beam focusing into the nozzle orifice. Ideally one would like to make the photolysis laser alignment parallel to the molecular beam, but system constraints do not readily allow this in practice. Timing for the experiments is controlled by using two synchronously timed Stanford Research Systems (SRS) digital delay generators (DG535). The timing precision is ∼3 ps, which is much less than the laser jitter of ∼2 ns. The use of the two SRS delay generators facilitates excellent temporal overlap between the excitation and ionization lasers. By using this setup, we also gain independent timing control over the nozzle and the photolysis laser so that we have more degrees of freedom by which to optimize the radical signal.

Excitation wavelengths for the radicals are generated using coumarin 440 or coumarin 460 in a Spectra Physics PDL-2 dye laser that is pumped with a 10-Hz Quanta Ray Nd:YAG laser. The mass-resolved excitation spectra (MRES) presented in this report are observed using ionization energy generated by doubling and mixing fluorescein 548 to generate 220-nm photons (∼45 455 cm^{-1}). This ionization energy is well in excess of the ionization threshold of both radicals by about 6000 cm^{-1}. Near-threshold ionization energies are generated using LDS 698 doubled and mixed with the Nd:YAG fundamental generating ∼252-nm photons (39 682 cm^{-1}). The mass spectroscopy and detection of the molecular ions is done in a time-of-flight mass spectrometer with a 1.5 m flight tube and a

10.1021/jp983457s CCC: $18.00
Published on Web 01/15/1999

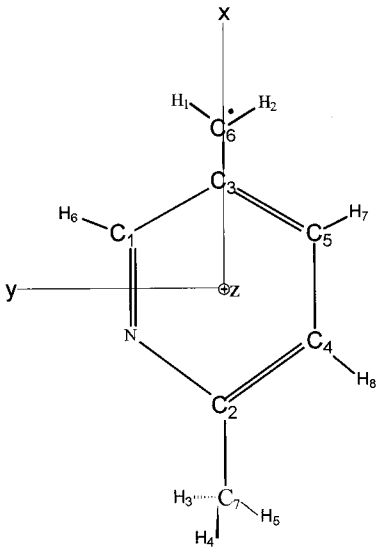

Figure 1. Coordinate reference for the 3-picolyl and 2,5-lutidyl radicals used for performing ab initio calculations. Due to the low C_s symmetry of the radical, only A′ and A″ irreducible representations can be identified. All in-plane modes ($\Delta Z = 0$) are of A′ symmetry, and all out-of-plane modes ($\Delta Z \neq 0$) are of A″ symmetry.

Galileo microchannel plate detector. Ion extraction voltages are set at 4.0, 3.75, and 0 kV on the separate extraction plates in the ionization region. The mass spectrometer calibration is determined by simultaneous observation of the 3-picoline and 2,5-lutidine precursor molecules for the 3-picolyl and 2,5-lutidyl radicals, respectively. Lifetimes are obtained by a standard laser pulse width/experimental decay deconvolution.

Calculational Procedures

Calculations presented in this paper are performed using two different ab initio programs: HONDO 8.5[12] and GAUSSIAN 94.[13] All calculations are performed on IBM Risc 6000 computers. To facilitate the calculations, a systematic process for doing them is employed. In all cases, a low-level ROHF ground-state calculation is performed in order to identify the orbitals to be used in the higher level complete active space (CAS) calculations. An optimal CAS calculation would include the orbitals for the conjugated π system on the ring and also the radical (n)p orbital located at the carbon in the meta position. As shown in Figure 1, we choose the z axis to coincide with these orbitals. For both picolyl and lutidyl radicals, this optimal CAS would require a (7 × 7) CAS (7 electrons, 7 orbitals) calculation; however, for some calculations, time and disk space prevent us from performing the optimal calculation. Several of the HONDO calculations are smaller than the optimal (5 × 5), but for these calculations, we also include a further step of an MP2 perturbation calculation to help adjust for any inaccuracies that might have occurred in choosing a smaller active space. Each excited-state calculation is checked to make sure that all the p_z orbitals are used for the calculation. The basis sets used for the calculations vary depending on the desired level of accuracy. All HONDO calculations are done using a Dunning−Huzinaga [9s/5p]/[3s/2p] double-ζ-plus polarization (DZP) basis set.[12] The calculations using GAUSSIAN 94 are performed utilizing the d95** basis set. These two basis sets are chosen so that the CAS accuracy for the calculations would be similar. Small basis sets are employed to check the qualitative accuracy of the calculations using the two different programs. Frequency calculations are performed using GAUSSIAN 94 and are only attempted after "tight" constraints are applied for the geometry optimization process. This, however, does not guarantee that a global minimum geometry is achieved. Because of the low symmetry of the species of concern, particularly the 2,5-lutidyl radical, the out-of-plane wagging motion of the methyl group presents some difficulty in the geometry optimization. The excited-state vibrational modes generated in this work often contain one negative energy (~ −75 cm^{-1}) involving the methyl group rotational motion of the 2,5-lutidyl radical. Six zero modes (±1.0 cm^{-1}) are calculated for this system. This "saddle-point" displacement is only found for the methyl rotation coordinate.

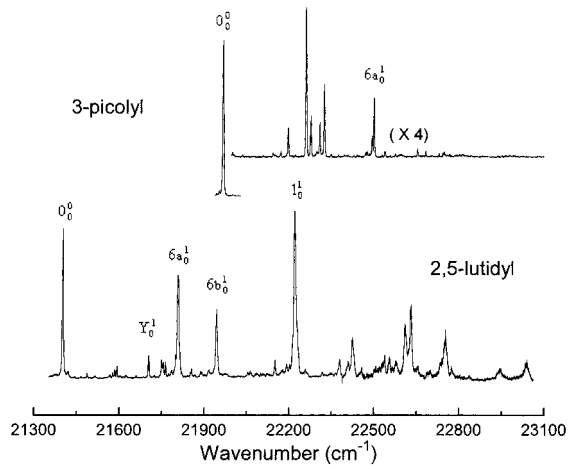

Figure 2. MRES of the 2,5-lutidyl and 3-picolyl radicals with origins at 21 395 and 21 965 cm^{-1}, respectively. All features of the 3-picolyl radical, except 0_0^0, have been increased by a factor of 4, indicating the nature of the poor Franck−Condon overlap for most vibronic states of the $D_1 \leftarrow D_0$ transition. See text for an elaboration of the vibronic assignments.

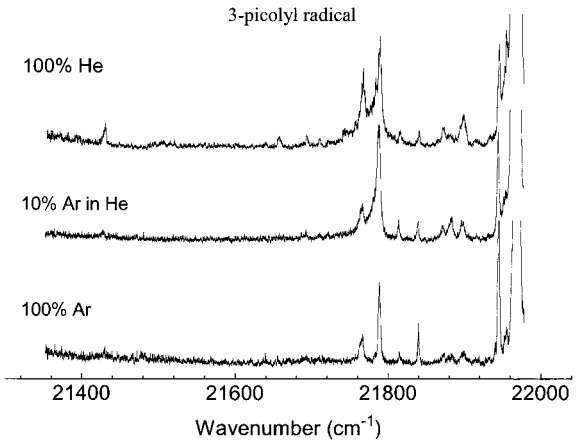

Figure 3. Addition of Ar to the backing gas to reduce the intensity of the hot bands in the spectra to the red of the 3-picolyl origin.

Results and Discussion

3-Picolyl Radical. The mass-resolved excitation spectrum for the picolyl radical is presented in Figure 2. Two features of the spectrum are of considerable importance for understanding the electronic properties of this radical. First, and most noticeably, is the lack of features beyond 0_0^0 + ~550 cm^{-1}. No distinguishable peaks are identified at higher energy. Similarly, the only lower energy features for ~1000 cm^{-1} are a few hot bands, observed if He is used as the backing gas. In Figure 3, an expanded region around the origin is shown to demonstrate the effects of adding different concentrations of argon to the molecular beam. As the peaks start to sharpen due to the enhanced cooling effect of argon, the relative intensities of the

TABLE 1: Picolyl Radical $D_1 \leftarrow D_0$ Transition Energies (in cm^{-1}). See Figures 2 and 4

vibronic energy	vibrational energy	assignment[a]
21 965.0	0	0_0^0
21 996.7	31.7	
22 033.9	68.9	
22 141.1	176.1	
22 268.4	203.4	
22 194.9	229.9	
22 259.2	294.2	
22 275.3	310.3	
22 296.2	331.2	
22 306.9	341.9	
22 322.6	357.6	
22 346.4	381.4	
22 469.7	504.7	
22 473.4	508.4	
22 491.8	526.8	$6a_0^1$
22 499.3	534.3	
22 536.4	571.4	

[a] Vibronic notation comes from the substituted benzene nomenclature as found in ref 14, for example.

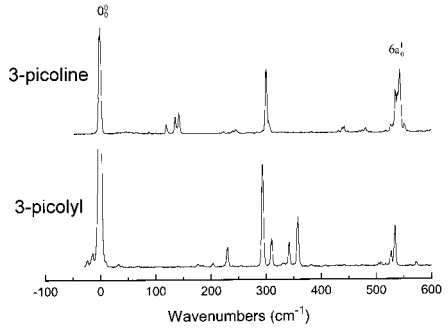

Figure 4. Comparison between the vibronic spectrum of the 3-picoline molecule and the 3-picolyl radical showing several features that are similar in energy. The most notable difference between the spectra is the large Franck−Condon factor for vibronic transitions of the molecule but not the radical. The spectra shown are relative to the 0_0^0 at 34 661 and 21 965 cm^{-1} of the molecule and radical, respectively.

peaks change, giving a good indication that these features are hot bands. Using 100% argon backing gas, the fwhm of the origin is ~2.8 cm^{-1}. The sharpness of this peak and the low hot band intensity are good indications that the radicals are well cooled in the expansion. Second, most of the intensity for the picolyl radical spectrum is in the first peak, the 0_0^0 transition at 21 965 cm^{-1}. We designate this feature the $\pi^* \leftarrow n(2p_z, C_\alpha)$ origin for the 3-picolyl radical. The origin intensity is approximately a factor of 5 larger than any other feature in the spectrum. (A list of all transitions is presented in Table 1.) This intensity profile for the transition suggests that the potential wells for the ground and excited states of the 3-picolyl radical are shifted very little from one another and, thus, the Franck−Condon factors for this radical transition are substantial only at the transition origin.

One of the constants in substituted benzyl systems is that the radical and precursor molecules have similar vibrational frequencies and vibronic spectra. An example of this similarity is found for the in-plane carbon symmetric bend mode referred to as 6a,b in the substituted benzene spectroscopy notation.[14] These modes have been shown for both closed-shell parent precursors and the associated radicals to be in the range ~400−650 cm^{-1} for both the ground and excited electronic states.[14a] The spectra of the 3-picoline molecule and the 3-picolyl radical are shown in Figure 4 to compare their observed vibronic structures. The 3-picoline molecule also exhibits little or no vibronic intensity beyond 600 cm^{-1} above the $\pi^* \leftarrow n$ transition origin; however, the intensity pattern for the features between 0 and 575 cm^{-1} above the origin is quite different for the two species. Nonetheless, some vibronic assignments can tentatively be made for the 3-picoline and 3-picolyl species based on the general knowledge of substituted benzene and pyridine vibronic spectra. The ν_6 degenerate in-plane carbon ring bending mode is split into a_1 and b_2 modes in C_{2v} symmetry.[15] The C_s symmetry of 3-picolyl and 2,5-lutidyl gives these two in-plane modes a′ symmetry. The 3-picoline molecule has a feature near $0_0^0 + 530$ cm^{-1} with an intensity similar to that of the origin, which we assign as $6a_0^1$; the relative intensity of the 0_0^0 and $6a_0^1$ transitions for 3-picoline is consistent with that found for other aromatic systems.[14] The picolyl spectrum has two peaks, one at 523 cm^{-1} and one at 534 cm^{-1}; we speculate that the more intense one (534 cm^{-1}) is the $6a_0^1$ vibronic feature. We make this speculation with some reservation because the intensity of this peak (relative to 0_0^0) is considerably less than that expected for this vibronically active mode.

TABLE 2: Lifetime Measurements for Several Related Organic Radicals

radical	lifetime	state
lutidyl	244.7 ns	0^0
picolyl	9.2 ns	0^0
benzyl	$\tau_s = 0.4$ μs, $\tau_1 = 1.3$ μs[a]	0^0
o-methylbenzyl	806 ns[b]	0^0
m-methylbenzyl	430 ns[b]	0^0
p-methylbenzyl	not measurable[b]	0^0
	1.43 μs	$0^0 + 351$ cm^{-1}
o-fluorobenzyl	420 ns[b]	0^0
m-fluorobenzyl	596 ns[b]	0^0
p-fluorobenzyl	532 ns[a]	0^0

[a] Lifetimes reported in ref 2. [b] Lifetimes reported in ref 1.

The lifetime of the excited D_1 electronic state of the 3-picolyl radical is investigated in an attempt to understand the lack of transition intensity beyond $0_0^0 + 550$ cm^{-1}. An exponential fit of the decay data for the 0_0^0 transition gives a lifetime of ~9 ns (see Table 2). This is close to the instrument resolution and is additionally confirmed by examining the fluorescence decay of the origin. This lifetime is about 100 times shorter than that of the benzyl radical analogue (see Table 2). This decrease in lifetime is not unexpected, as the same trend is observed for benzene and pyridine; however, this lifetime difference does not necessarily explain the absence of transition intensity beyond $0_0^0 + 500$ cm^{-1}. If lifetimes were the only consideration for transition intensity, one might expect the features to broaden and eventually lose intensity at higher energy levels; however, as noted previously, no identifiable features are observed above $0_0^0 + 575$ cm^{-1} even though the observed features are sharp to this energy.

Calculations for the 3-picolyl radical are in excellent agreement with both the experimental transition energy (within 1300 cm^{-1}) and also the ionization energy as shown in Tables 3 and 4, respectively. The ionization energy for the 3-picolyl radical is ~7.62 ± 0.03 eV. This is higher than that found for the benzyl radical based counterpart species and is consistent with the increase in the molecular ionization energy of methylpyridines with respect to toluenes.

2,5-Lutidyl Radical. The two-color mass-resolved excitation spectrum of the lutidyl radical is shown in Figure 2. An identical spectrum has also been observed in fluorescence but is not displayed here. The lutidyl radical's spectrum shows a single intense origin and three other features with considerable intensity. We attempt to assign these intense features based on

TABLE 3: Calculated and Observed Values for the $D_1 \leftarrow D_0$ Separations (cm^{-1}) for the Various Molecules of Interest in This Work (T_e = Calculated Electronic Difference; T_{00} = Observed Transition Energy)

radical	exptl T_{00}	theor T_e	theory level	basis set
benzyl	22 000	23 342	5 × 5 CASMP2[a]	DZP
3-picolyl	21 965	23 280	5 × 5 CASMP2[a]	DZP
2,5-lutidyl	21 395	22 804	7 × 7 CASSCF[b]	d95**
		23 007	7 × 7 CASSCF[b]	6-21G**
2-picolyl	N/A	22 445	5 × 5 CASMP2[a]	DZP
		23 072	7 × 7 CASSCF[b]	6-21G**
4-picolyl	N/A	24 309	5 × 5 CASMP2[a]	DZP
azepinyl	N/A	29 389	7 × 7 CASSCF[b]	d95**

[a] HONDO 8.5. [b] GAUSSIAN 94.

TABLE 4: Calculated Results for the Ionization Energies (IE in eV) of Different Radicals Important for This Work

	IE			
radical	exptl	theor	theory level	basis set
3-picolyl	7.6	7.36	ROHF[a]	DZP
2,5-lutidyl	7.3	6.76	7 × 7 CAS (gs)[b]	d95**
			6 × 6 CAS (ion)	d95**
2-picolyl		7.42	ROHF[a]	DZP
4-picolyl		7.36	ROHF	DZP
azepinyl		5.7	7 × 7 CAS (gs)[a]	DZP
			6 × 6 CAS (ion)	DZP

[a] HONDO 8.5. [b] GAUSSIAN 94.

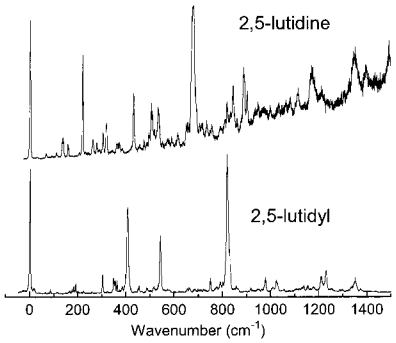

Figure 5. Spectra of 2,5-lutidine and 2,5-lutidyl radical relative to their respective origins at 34 563 and 21 395 cm^{-1}. The increased density of transitions in the 2,5-lutidine molecule is due to the double rotor states of the two methyl groups.

the vibrations of pyridines, as well as other conjugated systems with similar structure. Figure 5 shows a direct comparison between the vibronic spectra of 2,5-lutidine and the 2,5-lutidyl radical. All features in this radical spectrum are included in Table 5 along with assignments relating to the 0_0^0 and a few other possible vibrational modes. The intensities are not adjusted for laser power, but the dye laser power over the region between 0_0^0 and 1_0^1 (in-plane ring-breathing mode; see ref 15) is fairly constant using C460 as the laser dye.

Comparison of the lutidyl and benzyl radical spectra indicates some of the direct effects the nitrogen atom in the ring has on the vibronic spectrum and the D_1-D_2 state spacing and interaction. The lutidyl radical spectrum contains many features that are well resolved and has energy spacings that are indicative of a single electronic state without strong vibronic coupling from a second low-lying electronic state. Additional evidence for this interpretation is found in cluster studies of these radicals, which is to be reported in the following paper:[16] clusters with low binding energies are not observed at the high-energy vibronic features of the radical. If the high-energy vibronic peaks in this region were related to a second electronic state, as found for the benzyl radical, the clusters would start a second series of spectra built on the D_2 state. At even higher energy levels (>1200 cm^{-1}), the peaks start to broaden due to vibrational relaxation, couplings, and a high density of vibronic states.

TABLE 5: Lutidyl Radical $D_1 \leftarrow D_0$ Transition Energies (in cm^{-1})

vibronic energy	vibrational energy	assignment[a]
21 395.0	0	0_0^0
21 480.9	85.9	
21 508.6	113.6	
21 561.6	166.6	
21 570.9	175.9	
21 577.8	182.8	
21 586.7	191.7	
21 698.1	303.1	Y_0^1
21 743.6	348.6	
21 748.7	353.7	
21 757.8	362.8	
21 779.6	384.6	
21 801.5	406.5	$6a_0^1$
21 849.7	454.7	
21 881.1	486.1	
21 909.7	514.7	
21 938.5	543.5	$6b_0^1$
22 056.4	661.4	
22 145.4	750.4	
22 214.6	819.6	1_0^1
22 252.3	857.3	
22 373.2	978.2	
22 418.1	1023.1	
22 533.4	1138.4	
22 550.1	1155.1	
22 573.1	1178.1	
22 603.7	1208.7	
22 624.4	1229.4	$1_0^1 + 6a_0^1$
22 746.5	1351.5	$1_0^1 + 6b_0^1$
22 936.6	1541.6	
23 031.9	1636.9	

[a] See ref 15. Notation is that for substituted benzene ring modes. ν_1 is the totally symmetric D_{6h} ring breathing in-plane carbon mode. ν_{6a} and ν_{6b} are discussed in the text.

In addition to the spectra, we present calculational results in Table 3, which are in very good agreement with the measured origin transition. Using GAUSSIAN 94, the d95** basis set, and a (7 × 7) CAS algorithm that includes the p orbital of the radical electron and the π orbitals of the ring as discussed earlier, the calculated transition energy for the 0_0^0 of 2,5-lutidyl is 22 804 cm^{-1}. This calculated value is within 1500 cm^{-1} of the measured value. Frequency calculations for the lutidyl radical are presented in Table 6. Calculations for both the ground- and excited-state geometries are shown along with ground-state vibrations for the 2,5-lutidine molecule. The frequencies presented correspond to the a′ and a″ modes of the pyridine ring. The a′ modes are in-plane vibrations, whereas the a″ modes are out-of-plane modes. Normal modes that involve the methyl group and the radical carbon have been left out. For the excited-state modes, three calculated vibrations are found below 1000 cm^{-1} that are attributed to the radical and methyl group motion: these energies are 300, 339, and 465 cm^{-1}. By using a correlation table to compare the modes of the C_{2v} pyridine chromophore with the C_s symmetry of the lutidyl radical, we are able to assign several of the peaks as shown in Figure 5. The feature at 303 cm^{-1} is assigned as Y_0^1, that is, the vibronic mixing state of two out-of-plane modes referred to as 10a and 16a in the benzene notation.[14,15a,b] The coupling between these two states is evident in pyridine gas-phase studies.[17]

TABLE 6: Calculated Vibrational Energies for the Ground and Excited States of the 2,5-Lutidyl Radical Omitting the Methyl Hydrogen Atoms. Comparisons Are Given by Listing the Corresponding 2,5-Lutidine Ground State Vibrational Energies (All Values in cm^{-1})

	lutidyl		
mode[a]	D_1	D_0	lutidine S_0[b]
a′			
ν_1	3387	3384	3065
ν_2	3363	3362	3021
ν_3	3341	3353	3009
ν_4	1748	1672	1601
ν_5	1623	1619	1567
ν_6	1573	1507	1490
ν_7	1494	1412	1450
ν_8	1450	1355	1320
ν_9	1378	1321	1294
ν_{10}	1337	1256	1245
ν_{11}	1273	1170	1216
ν_{12}	1213	1095	1138
ν_{13}	1026	1079	1031
ν_{14} (1)	830	876	844
ν_{15}	739	786	727
ν_{16} (6b)	646	684	647
ν_{17} (6a)	480	479	479
ν_{18}	397	392	392
ν_{19}	301	313	295
a″			
ν_{20}	1008	1090	964
ν_{21}	910	939	920
ν_{22}	710	905	815
ν_{23}	633	764	695
ν_{24}	423	524	485
ν_{25}	293	425	409
ν_{26}	179	326	319
ν_{27}	79	139	147

[a] Assignments in parentheses are based on mode patterns which suggest $D_{6h} \rightarrow C_{2v}$ similarities. The correlation is very difficult for this low symmetry molecule as all a′ and all a″ modes mix to a considerable extent. Mode energies also assist in this correspondence. [b] See ref 19.

Replacement of a carbon atom in the conjugated ring system by a nitrogen atom has a significant affect on the lifetime of the radical. The lifetime measurements for the electronic origins of benzyl and substituted-benzyl radicals are compiled and presented in Table 2. The presence of the nitrogen atom in the ring has reduced the excited-state lifetime by nearly a factor of 2 for lutidyl with respect to xylyl. The presence of nitrogen in the ring does two things: reduces the approximate symmetry of the molecule and adds a lone pair of electrons to the system. On the other hand, the picolyl radical in the D_1 state has a lifetime of only ~9 ns. It is somewhat counterintuitive that an increase in the density of states, brought about by replacing a hydrogen atom with a CH_3 group, should increase the excited-state lifetime. Clearly, this demonstrates that the addition of the CH_3 group eliminates a mechanism by which the 3-picolyl radical undergoes relaxation to the ground state: perhaps some resonance between the D_0 and D_1 states is thereby broken.

The ionization energy for the 2,5-lutidyl radical is found to be approximately 7.33 ± 0.03 eV. The increase in the ionization energy of this pyridine-derived radical compared to benzyl radicals is consistent with the increase of the ionization energy for the 2,5-lutidine molecule with respect to its xylene analogues (see Table 4).

2- and 4-Picolyl and the Remaining Lutidyl Radicals. Using the same techniques described above to generate the 3-picolyl and 2,5-lutidyl radicals, the 2- and 4-picolyl radicals or any of the associated lutidyl radicals could not be detected. In an attempt to understand why these radicals cannot be observed by gas-phase photolysis or pyrolysis,[14a] an extensive series of ab initio calculations were undertaken. These calculations are primarily limited to picolyl radicals because they are less computationally expensive than their lutidyl counterparts. HONDO 8.5 and GAUSSIAN 94 are used to facilitate the calculations presented in this work. Calculations done with HONDO use Dunning's (9s,5p)/(3s,2p) basis set, plus additional polarization functions (DZP).[12] The HONDO complete active space (CAS) calculations are based on a 5×5 active space, which includes the radical electron orbital and the π orbitals that are perpendicular to the plane of the ring. The nitrogen lone pair is "frozen" in all calculations to ease the computational strain of delocalizing the lone pair over the rest of the molecular ring. The results of these calculations are listed in Table 3 along with comparable values for the benzyl radical. Also listed in Table 4 are the calculated ionization energies using the restricted open-shell Hartree−Fock (ROHF) algorithm and the basis sets listed for the picolyl radicals. The ionization energy values reported for lutidyl and the seven-membered-ring azepinyl radical, discussed below, are based on calculations using a (7×7) CAS for the ground state and a (6×6) CAS for the ion. The calculated values, both the excitation energy and the ionization potential, for the 3-picolyl radical correspond very well to their experimental values discussed above. Based on the accuracy of the 3-picolyl, 2,5-lutidyl, and the corresponding benzyl radical calculations, we are confident that the results for the 2- and 4-picolyl radicals are reasonable. Based solely on the results of the transition energies, these calculations suggest that all of the picolyl radicals should have been accessed by our experimental techniques and scanning ranges.

The effects of conjugation on the stability of these radicals can also be considered as the resonance structures differ for the 2-, 3-, and 4-picolyl radicals. The 2- and 4-picolyl radicals have resonance structures that position the radical electron on the nitrogen atom, whereas the 3-picolyl radical does not. One speculation is that the radical is more stable at the nitrogen site: this could provide an explanation for why these radicals are not observed as the $\pi^* \leftarrow$ n radical electron transition would be at a different energy. Nonetheless, thorough examination of the orbitals generated by the CAS and CASMP2 calculations shows that the excitation is primarily localized at the $(n)p_z$ orbital on the CH_2. This observation is further substantiated by the similar transition energies (see Table 4) for all radicals (picolyl, lutidyl, and benzyl) discussed in this comparison. These observations further support the notion that resonance structure differences are not responsible for the fact that the other isomeric radicals could not be detected in these studies.

Rearrangement. Rearrangement of the picoline molecule to form aniline in both 2- and 4-picoline solutions and in the gas phase, using a photoexcitation energy higher than 253 nm, has been observed.[18] By using 193 nm as the photolysis wavelength, we have been able to observe a significant increase in the amount of aniline signal using all three picoline precursors. Unfortunately, a quantitative determination of the amount of aniline produced is not possible due to the differing vapor pressures for each of the three starting compounds.

As a result of this observation, one can speculate that these benzyl-like radicals rearrange to form a seven-membered (azepine) ring radical, the azepinyl radical. The formation of the seven-membered ring requires a ring expansion, as well as a 1,2-hydrogen shift to form a conjugated allyl-type ring radical. Such an azepinyl radical is believed to be an intermediate in the rearrangement of phenylnitrene to form cyanocyclopenta-

dienyl.[20] In an effort to determine the credibility of this assumption, we again utilize calculations. The results of these calculations are presented in Table 3. A (7 × 7) CAS algorithm is employed to calculate the transition energy for the azepinyl radical. Again, p_z orbitals are chosen assuming an $n \rightarrow \pi^*$ transition. The calculations show that the $D_1 \leftarrow D_0$ electronic transition origin is somewhat higher in energy than that for the corresponding picolyl structures. As shown in Table 3, (5 × 5) CASMP2 and (7 × 7) CASSCF calculations generate quite comparable transition energies for these systems. The main calculational difference between the two different isomeric structures (six- vs seven-membered rings) is found in the ionization energies (see Table 4). The ionization energies for the substituted pyridine ring structures are ~7.4 eV compared with that for the seven-membered ring structure, which is ~5.7 eV. On the basis of the results for the calculated ionization energy for the 2,5-lutidyl radical, we can suggest that this value is low by as much as 0.6 eV or ~5000 cm^{-1}. Nevertheless, the azepine ring structure for a rearranged lutidyl or picolyl radical would surely have been detected if its excited-state lifetime were greater than ca. 50 ps. One possibility is that the missing radicals are present in the ground-state D_0 species, but upon optical excitation, they rapidly rearrange to the azepine structure.

Conclusion

Using both mass-resolved excitation and fluorescence excitation spectroscopy, two previously undetected radicals, the 3-picolyl radical and the 2,5-lutidyl radical, are isolated and studied. These radicals show both similarities with and differences from their benzyl radical analogues. The excited-state lifetimes of these newly characterized heterocyclic radicals are much shorter than those of their benzyl radical counterparts, and the addition of a nitrogen atom to the ring increases the ionization energy of the radicals. The lifetime difference between the picolyl radical and the benzyl radical approaches a factor of 100. Addition of a second methyl group to the pyridine ring to form the lutidyl radical again decreases the lifetime but now only by a factor of 10 with respect to that of the benzyl radical. These lifetime decreases upon methyl substitution can be compared with the factor of 2 decrease observed for the xylyl radical compared to the benzyl radical. This decrease in lifetimes suggests that the addition of the CH_3 methyl group to the picolyl radical to form the lutidyl radical eliminates or significantly alters a nonradiative decay pathway present in the picolyl radical. The D_2 excited state of the picolyl and lutidyl radicals is not near the D_1 state as is found for the benzyl radical.

Ab initio calculations for the observed radicals are in excellent agreement with experimental results. The transition energies and ionization energies calculated are in good agreement with the experimental results for $D_1 \leftarrow D_0$ transition and ionization energies for both species. The calculations suggest that ring expansion through a seven-membered ring (azepine) structure could account for the missing 2- and 4-picolyl radicals and their lutidyl counterparts if the lifetimes for the excited-state D_1 species are short.

Acknowledgment. We thank Dr. David P. Taylor for his assistance with the initial calculations and experiments for these studies. This effort is supported in part by grants from the USNSF and USARO.

References and Notes

(1) Charlton, T. R.; Thrush, B. A. *Chem. Phys. Lett.* **1986**, *125*, 547.
(2) Fukushima, M.; Obi, K. *J. Chem. Phys.* **1990**, *93*, 8488.
(3) Hoffbauer, M. A.; Hudgens, J. W. *Chem. Phys. Lett.* **1985**, *89*, 5152.
(4) (a) Cossart-Magos, C.; Leech, S. *J. Chem. Phys.* **1976**, *64*, 4006. (b) Cossart-Magos, C.; Leach, S. *J. Chem. Phys.* **1972**, *56*, 1534.
(5) Orlandi, G.; Poggi, G.; Zerbetto, F. *Chem. Phys. Lett.* **1985**, *115*, 253.
(6) (a) Eiden, G. C.; Weisshaar, J. C. *J. Chem. Phys.* **1996**, *104*, 8896. (b) Eiden, G.; Weisshaar, J. C. *J. Phys. Chem.* **1991**, *95*, 6194. (c) Eiden, G.; Weinhold, F.; Weisshaar, J. C. *J. Chem. Phys.* **1991**, *95*, 8665. (d) Eiden, G.; Lu, K.-T.; Badenhoop, J.; Weinhold, F.; Weisshaar, J. *J. Chem. Phys.* **1996**, *104*, 8886.
(7) (a) Tai-Yuan, D. L.; Miller, T. A. *J. Phys. Chem.* **1990**, *94*, 3554. (b) Foster, S. C.; Miller, T. A. *J. Phys. Chem.* **1989**, *93*, 5986 and references therein. (c) Li, T. D.; Tan, X.; Cerny, T. M.; Williamson, J. M.; Cullin, D. W.; Miller, T. A. *Chem. Phys.* **1992**, *203*, 167. (d) Lin, T. D.; Miller, T. A. *J. Phys. Chem.* **1990**, *94*, 3554. (e) Lin, T. D.; Damo, C. P.; Dunlop, J. R.; Miller, T. A. *Chem. Phys. Lett.* **1990**, *168*, 349.
(8) Mochizuki, Y.; Kaya, K.; Ito, M. *Chem. Phys.* **1981**, *54*, 375.
(9) Walker, I. C.; Palmer, M. H.; Kopkirk, A. *Chem. Phys.* **1989**, *141*, 365.
(10) Villa, E.; Amirav, A.; Lim, E. C. *J. Phys. Chem.* **1988**, *92*, 5393.
(11) (a) Disselkamp, R.; Bernstein, E. R. *J. Chem. Phys.* **1993**, *98*, 4339. (b) Im, H. S.; Bernstein, E. R. *J. Chem. Phys.* **1991**, *95*, 6326. (c) Disselkamp, R.; Bernstein, E. R. *J. Phys. Chem.* **1994**, *98*, 7260. (d) Bray, J. A.; Bernstein, E. R. Unpublished.
(12) (a) Dupuis, M.; Farazdel, A. HONDO (IBM Corp., Center for Scientific and Engineering Computations, Kingston, NY, 1990). (b) *Methods of Electronic Structure Theory*; Dunning, T. H., Hayes, P. J., Schaefer, H. F., III, Eds.; Plenum: New York, 1977; Vol. 3, p 1.
(13) Gaussian 94, Frisch, M. J.; Trucks, G. W.; Schlegel, H. B.; Gill, P. M. W.; Johnson, B. G.; Robb, M. A.; Cheeseman, J. R.; Keith, T. A.; Peterson, G. A.; Montgomery, J. A.; Raghavachari, K.; Al-Laham, M. A.; Zakrzewski, V. G.; Ortiz, J. V.; Foresman, J. B.; Cioslowski, J.; Stefanov, B. B.; Nanayakkara, A.; Challacombe, M.; Peng, C. Y.; Ayala, P. Y.; Chen, W.; Wong, M. W.; Andres, J. L.; Replogle, E. S.; Gomperts, R.; Martin, R. L.; Fox, D. J.; Binkley, J. S.; Defrees, D. J.; Baker, J.; Stewart, J. P.; Head-Gordon, M.; Gonzales, C.; Pople, J. A. Gaussian, Inc.; Pittsburgh, PA, 1995.
(14) (a) Yao, J.; Bernstein, E. R. *J. Chem. Phys.* **1997**, *107*, 3352. (b) Nimlos, M. R.; Young, M. A.; Bernstein, E. R.; Kelley, D. F. *J. Chem. Phys.* **1989**, *91*, 5268. (c) Chernoff, D. A.; Rice, S. A. *J. Chem. Phys.* **1979**, *70*, 2521 and references therein.
(15) (a) Wilberg, K. B.; Walters, V. A.; Wong, K. N.; Colson, S. D. *J. Phys. Chem.* **1984**, *88*, 6067. (b) Ajito, K.; Takahashi, M.; Ito, M. *Chem. Phys. Lett.* **1989**, *158*, 193. (c) Draeger, J. A. *Spectrochim. Acta* **1983**, *39A*, 809. (d) Green, J. H. S.; Harrison, D. J.; Kynaston, W.; Paisley, H. M. *Spectrochim. Acta* **1970**, *26A*, 2139.
(16) Bray, J. A.; Bernstein, E. R. *J. Phys. Chem.* **1998**, *102*, following paper in this issue.
(17) Mochizuki, Y.; Kaya, K.; Ito, M. *J. Chem. Phys.* **1976**, *65*, 4163.
(18) Kraus, M.; Roszakt, S. *J. Mol. Spectrosc.* **1994**, *310*, 155.
(19) Green, J. H. S.; Harrison, D. J.; Kynaston, W.; Paisley, H. M. *Spectrochim. Acta* **1970**, *26A*, 2139.
(20) Im, H. S.; Bernstein, E. R. *J. Chem. Phys.* **1991**, *95*, 6326.